Supplementary Figures and Table

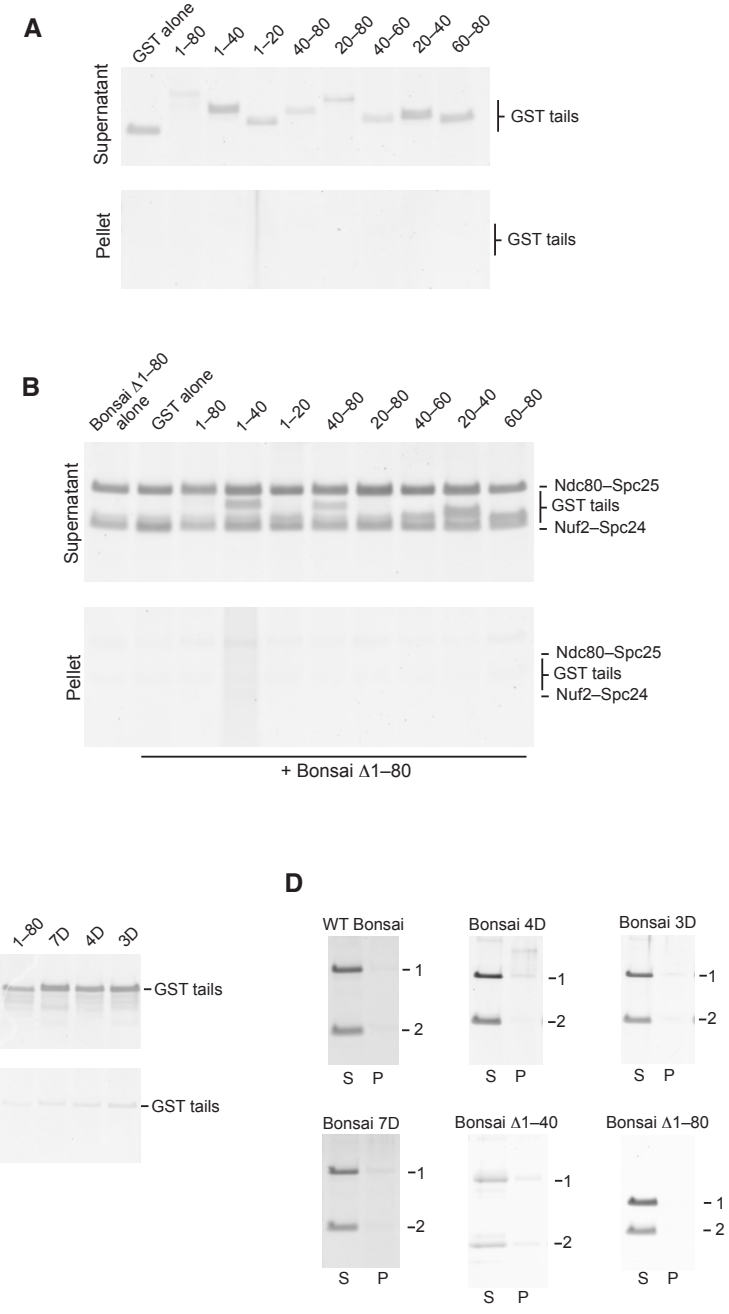

Supplementary Figure 1. Self-pelleting controls of GST tail and Ndc80 bonsai constructs

SDS-PAGE of sedimentation experiments in identical conditions to the experiments in: A) Fig. 1d, B) Fig. 1e, C) Fig. 2b, D) Fig. 2d, except in the absence of microtubules. None of the constructs showed significant self-pelleting.

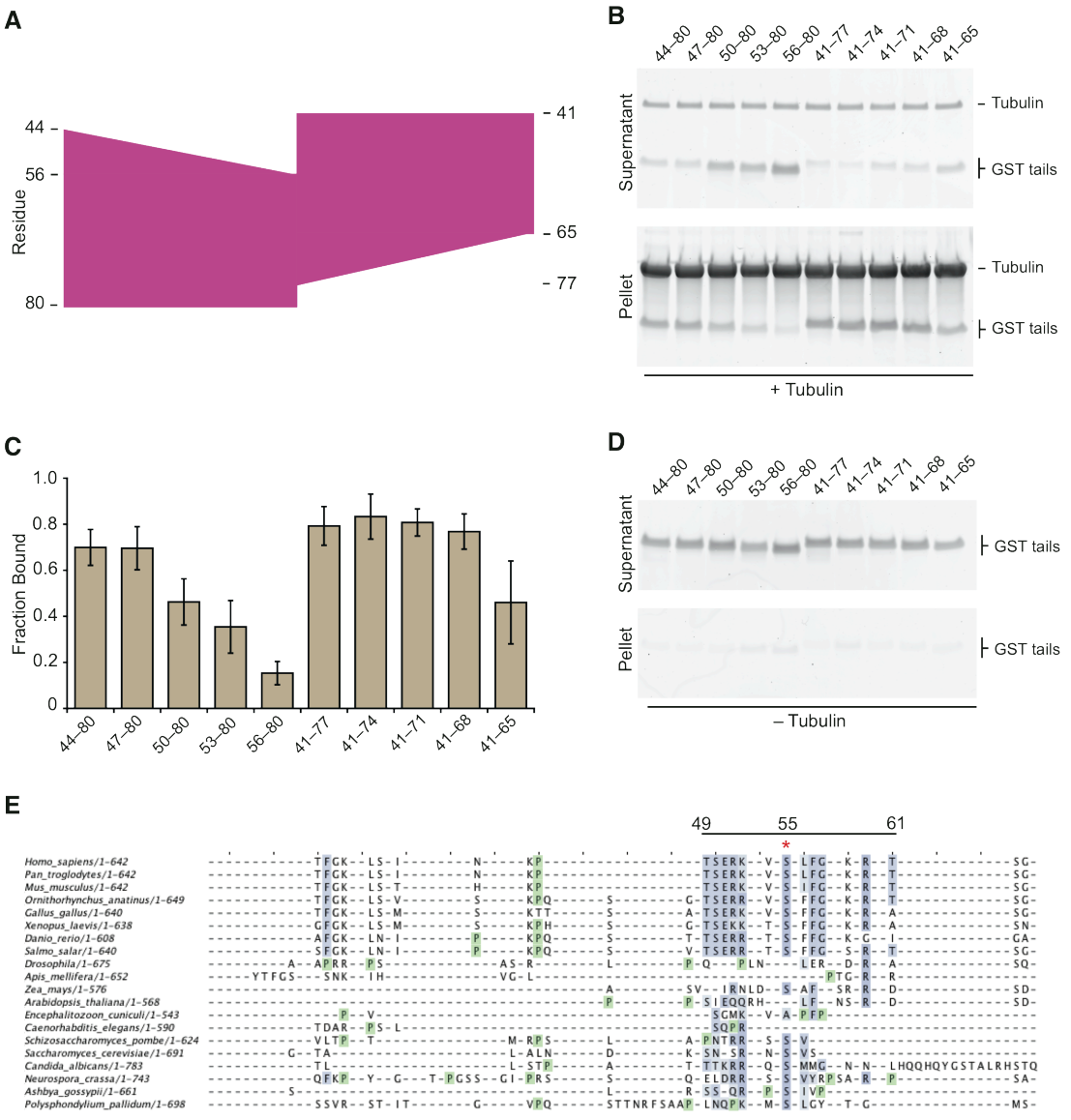

Supplementary Figure 2. Delineation of the minimal tubulin-binding region of the Ndc80 tail

A) Schematic diagramming the constructs used in the experiments presented in B–C. Truncations were made in 3 amino-acid steps. B) SDS-PAGE of microtubule co-sedimentation assays with GST tail constructs. Tubulin, 3 µM, GST tails, 1 µM. C) Quantification of B. Error bars represent s.d., *n* = 3. D) SDS-PAGE of sedimentation experiment as in B, but in the absence of microtubules. E) Multiple sequence showing representative species. Areas of modest conservation are indicated in blue, prolines are indicated in green. The minimal tubulin binding region is relatively conserved, and features one highly conserved Aurora B site, indicated with red asterisk. The full alignment was of 136 sequences, performed with T-COFFEE.

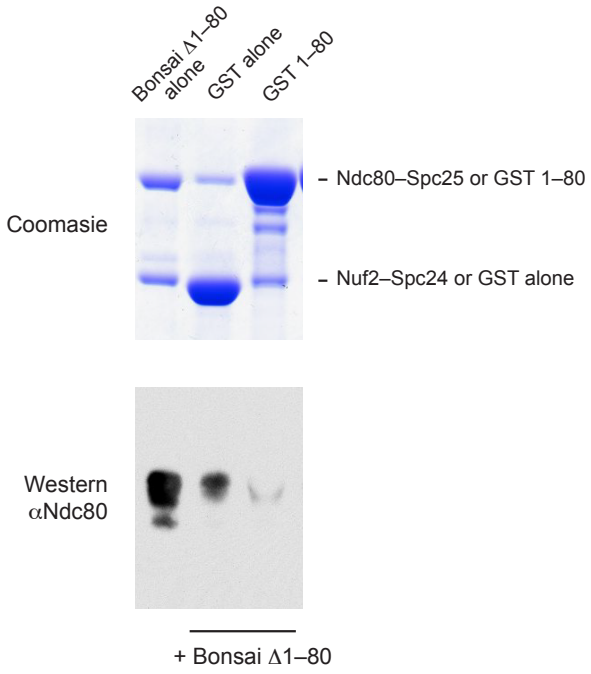

Supplementary Figure 3. The Ndc80 tail does not interact with the Ndc80 globular head in trans in the absence of microtubules

GST pull-down experiment, where the GST 1–80 tail construct or GST alone was mixed with bonsai Δ1–80. In the absence of GST, bonsai Δ1–80 interacts non-specifically with glutathione resin. This interaction is actually reduced when either GST alone or GST 1–80 is present, suggesting that there is no detectable interaction between the tail and the Ndc80 globular domain in the absence of microtubules.

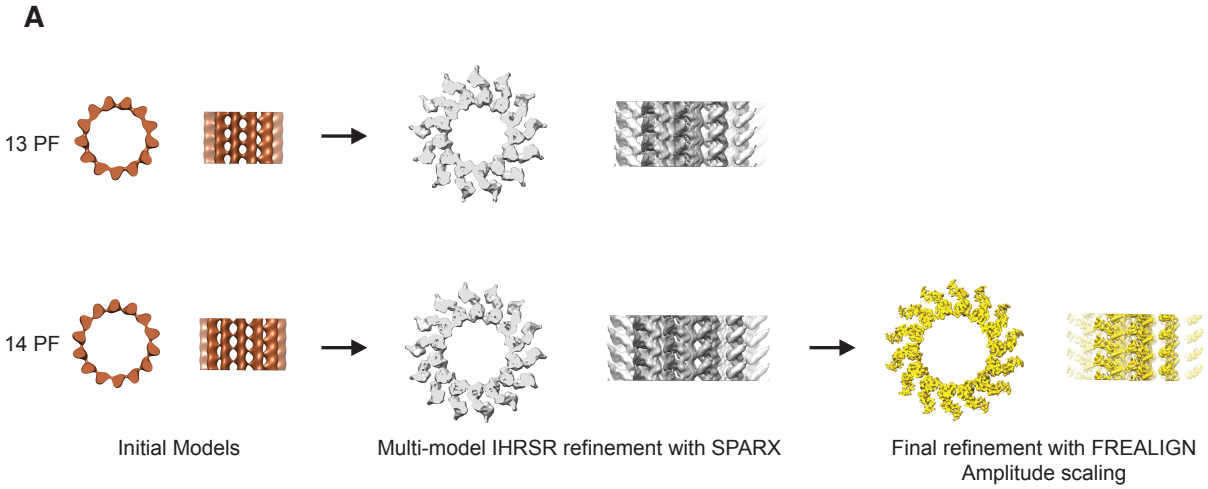

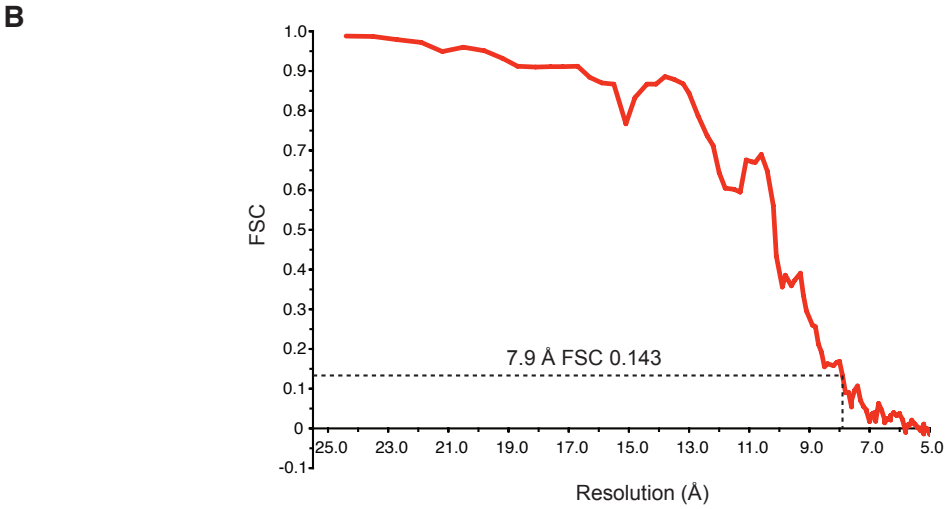

Supplementary Figure 4. Improved cryo-EM reconstruction of the Ndc80–microtubule interface.

A) Outline of the reconstruction process. The multi-model refinement strategy allowed a larger fraction of the data reported in ref. 23 to be aligned, and resulted in significantly improved resolution**.** The 14pf mictotubule, which represented a larger fraction of the data, was chosen for high-resolution refinement with FREALIGN. B) Assessment by the Fourier Shell Correlation 0.143 criterion suggests a resolution of 7.9 Å.

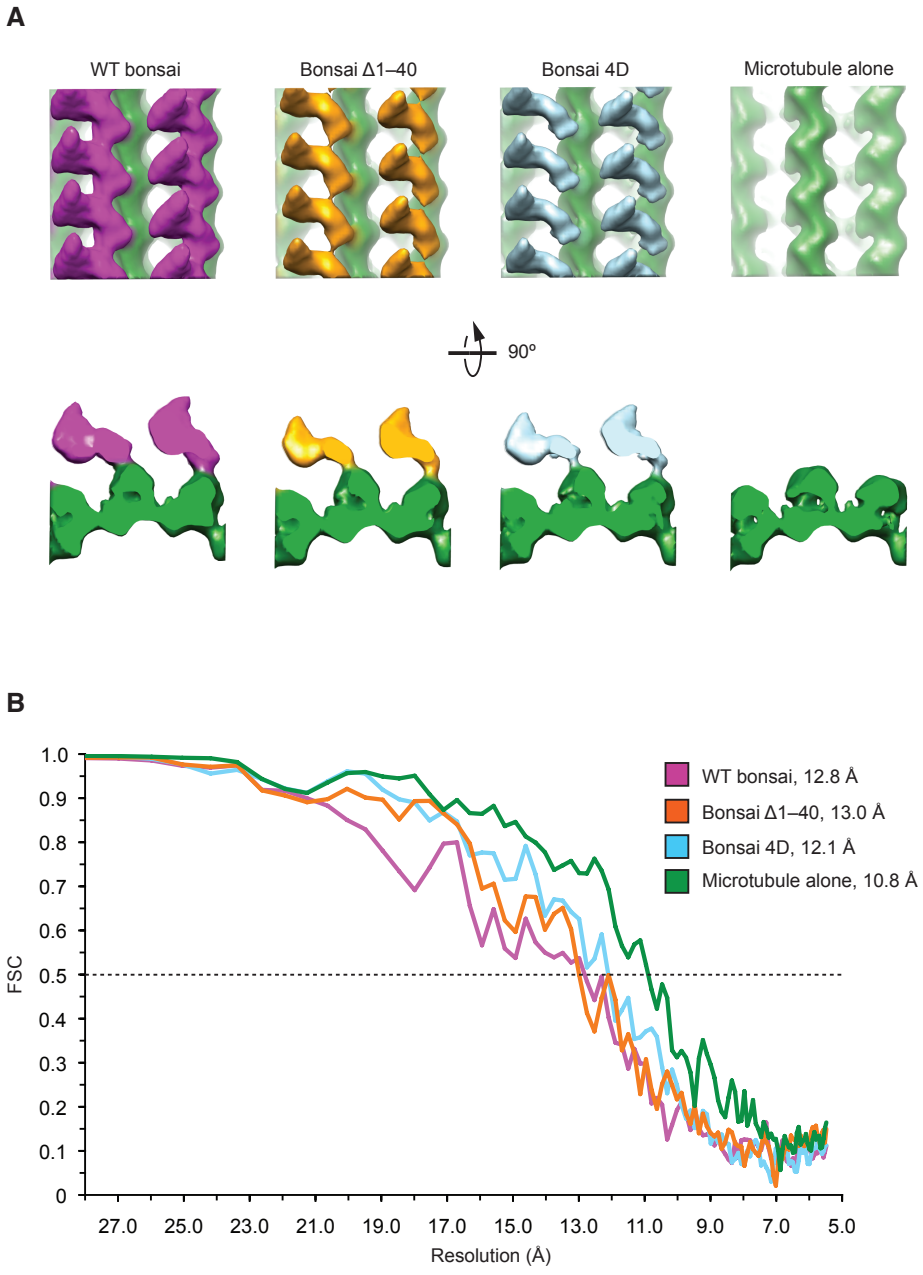

Supplementary Figure 5. Cryo-EM reconstructions of bonsai mutants for difference map calculation

A) Isosurface renderings of the 4 different reconstructions required for difference map calculation, contoured so that tubulin occupies equal volume. Note that the mutant bonsai constructs appear to be sub-stoichiometric, necessitating pre-subtraction of the microtubule for difference map analysis between the mutants and the wild-type. B) Assessment by the Fourier Shell Correlation 0.5 criterion shows all reconstructions have a resolution better than 13 Å.

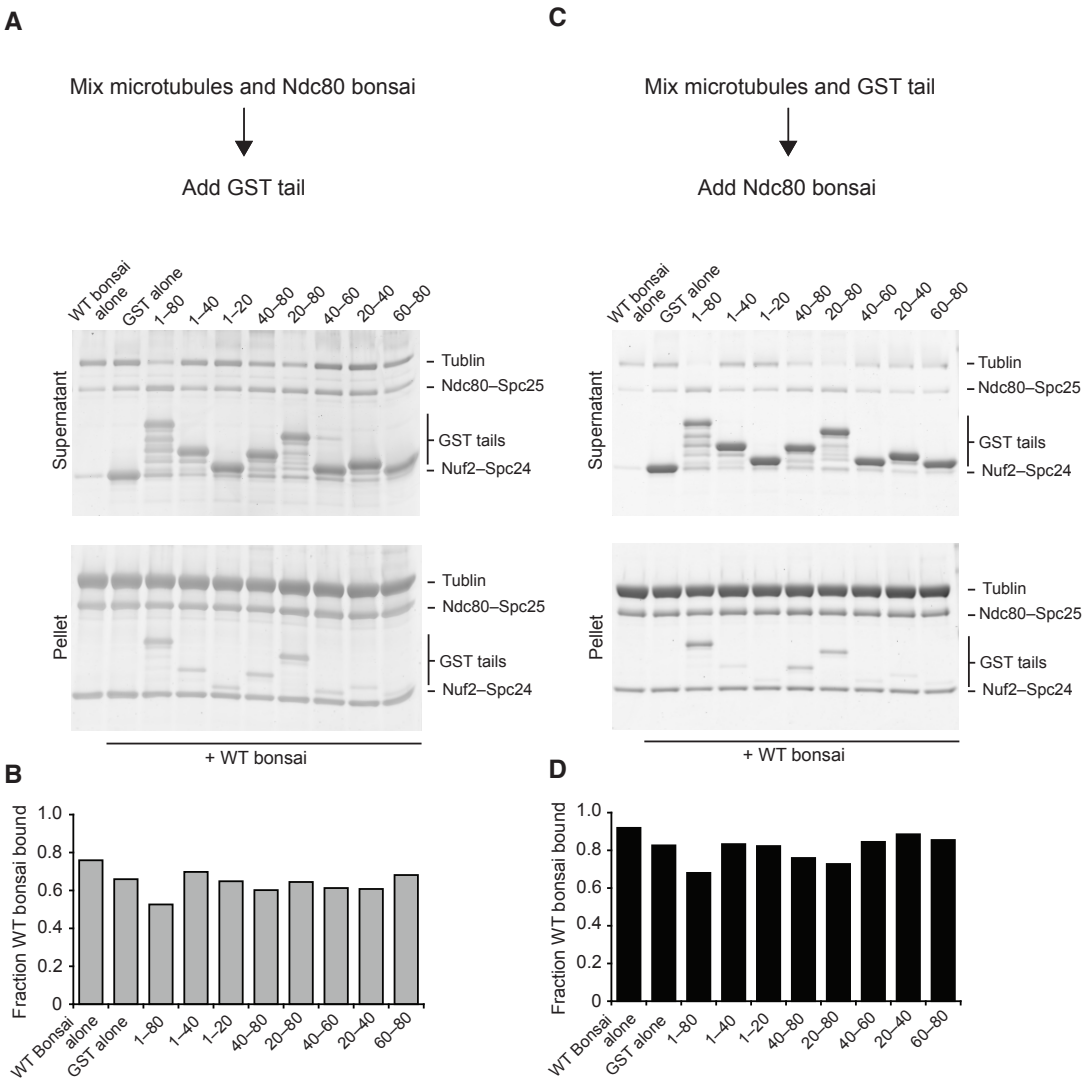

Supplementary Figure 6. The Ndc80 bonsai outcompetes the Ndc80 tail for microtubule binding

A) SDS-PAGE of competition microtubule co-sedimentation experiment where GST-tails and microtubules were premixed. Tubulin, 1 µM, GST tails, 1 µM, wild-type bonsai 0.5 µM. B) Quantification of A, $n = 1$. C) SDS-PAGE of competition microtubule co-sedimentation experiment where wild-type bonsai and microtubules were premixed. D) Quantification of E, $n = 1$. Since the order of addition does not affect the outcome of the experiment, equilibrium is reached and the full bonsai complex outcompetes the N-terminal tail despite the tail being in excess.

	Bonsai Δ1–80	Bonsai 7D	Bonsai Δ1–40	Bonsai 3D	Bonsai 4D
WT	8.8×10^{-12}	3.1×10^{-12}	3.0×10^{-3}	8.2×10^{-7}	2.2×10^{-7}
Bonsai Δ1–80		6.1×10^{-1} ***	3.7×10^{-7}	1.2×10^{-3}	6.1×10^{-4}
Bonsai 7D			1.1×10^{-7}	3.7×10^{-4}	1.4×10^{-4}
Bonsai Δ1–40				1.8×10^{-2}	7.5×10^{-3}
Bonsai 3D					8.2×10^{-1} ***

Supplementary Table 1. Pairwise statistical comparisons between cluster distributions

P values from Welch's t-tests between the distributions shown in Fig. 3c. The comparisons bonsai 7D vs. bonsai Δ1–80 and bonsai 3D vs. bonsai 4D both give *P* values greater than α(0.05), indicated by asterisks.

Supplementary Movie1 - Cryo-EM structure of the Ndc80–microtubule interface

Supplements Fig. 5A. Crystal structures of two bonsai Δ1–80 molecules (PDB 2VE7) and tubulin (PDB 1JFF) docked into the improved cryo-EM density map, colored as in Fig. 5A. Two densities not occupied by the crystal structures (magenta) were interpreted as corresponding to ordered regions of the N-terminal tail.

Supplementary Movie2 - Visualizing the Ndc80–E hook interface

Supplements Fig. 5C. Same as Supplementary Movie1, but with the cryo-EM map displayed at a lower threshold, where the tubulin E hooks (red) are visible.